Electronic Supplementary Material (ESI) for Nanoscale.
This journal is © The Royal Society of Chemistry 2023

Electronic Supplementary Information (ESI) for Nanoscale. This journal is © The Royal Society of Chemistry 2022

Electronic Supplementary Information

Strong interlayer coupling and unusual antisite defects mediated p-type conductivity in GeP_x (x = 1, 2)

Guoxujia Chen[a], Weiwei Meng[b*], Xiaoxi Guan,[a] Peili Zhao,[a] Shuangfeng Jia[a], He Zheng[acd], Dongshan Zhao[a*], and Jianbo Wang[ae*]

a. School of Physics and Technology, Center for Electron Microscopy, MOE Key Laboratory of Artificial Micro- and Nano-structures, and Institute for Advanced Studies, Wuhan University, Wuhan 430072, China
b. South China Academy of Advanced Optoelectronics, South China Normal University, Guangzhou 510006, China
c. Suzhou Institute of Wuhan University, Suzhou, Jiangsu 215123, China
d. Wuhan University Shenzhen Research Institute, Shenzhen, Guangdong 518057, China
e. Core Facility of Wuhan University, Wuhan 430072, China

Corresponding Author

*Email: wang@whu.edu.cn; dszhao@whu.edu.cn; meng@whu.edu.cn.

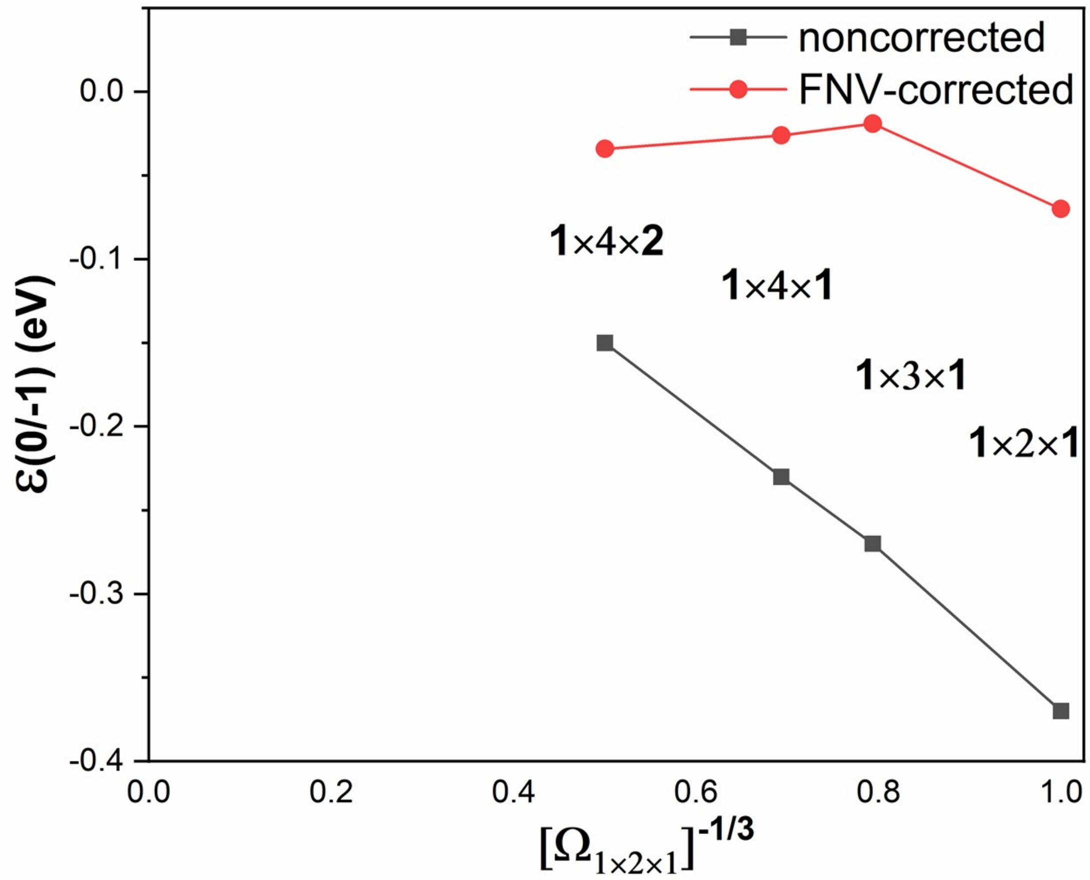

Figure S1. The transition energy level of P vacancy, ε(0/-1), calculated with varied volume Ω (in unit of volume of 1×2×1 supercell, $\Omega_{1\times2\times1}$) of supercells in bulk GeP.

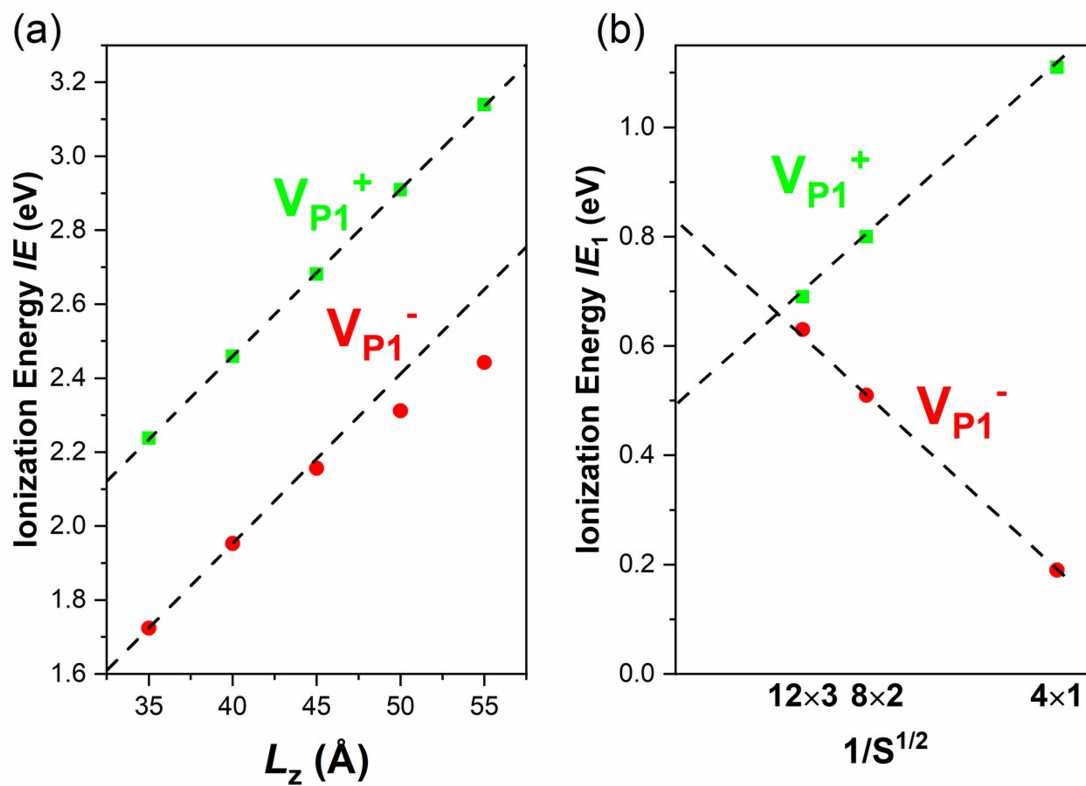

Figure S2. Transition energy level (ionization energy) ε(+1/0) and ε(0/-1) of P vacancy as a function of (a) the length of the slab in the z-direction and (b) $1/S^{1/2}$ (S: the lateral size of slab).

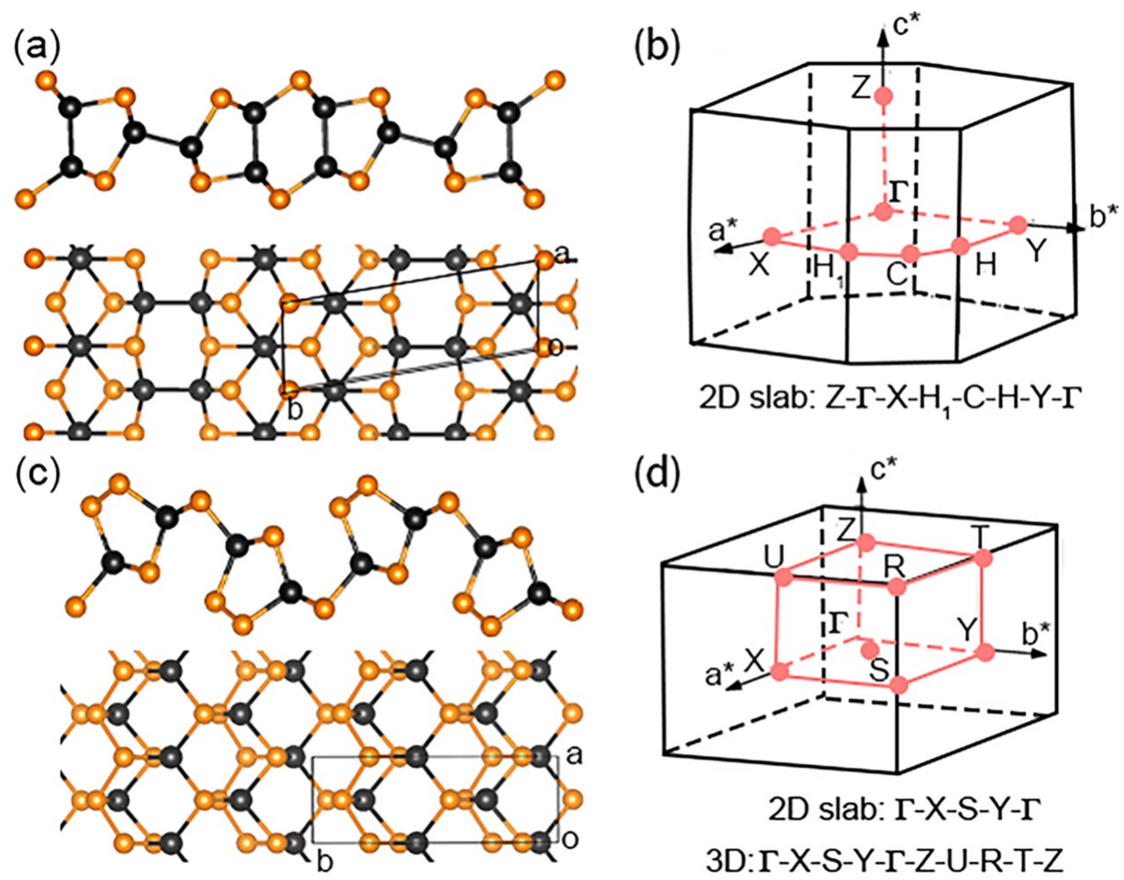

Figure S3. (a) Structures of 1L GeP and (b) high-symmetry path of k-points in the reciprocal space, (c) structures of 1L GeP_2 and (d) high-symmetry path of k-points in the reciprocal space.

Table S1. Theoretical lattice constants (*a*), bandgaps (E_g) of GeP and GeP_2 with experimental values or calculated results for comparison.

		a (Å)	*b* (Å)	*c* (Å)	*β* (°)	E_g (eV)		ΔE_g (eV)
						bulk	1L	E_g^{1L}-E_g^{bulk}
GeP	This work	15.36	3.71	9.31	79.28	1.07	2.39	1.32
	Theo.[10]	15.86	3.70	9.33	79.24	0.94	2.31	1.37
	Exptl.[32,33]	15.14	3.64	9.19	78.90	0.9	2.3	1.4
GeP_2	This work	3.57	10.18	14.35	90	1.65	2.01	0.36
	Theo.[34]	3.54	10.40	14.52	90	-	1.98	-

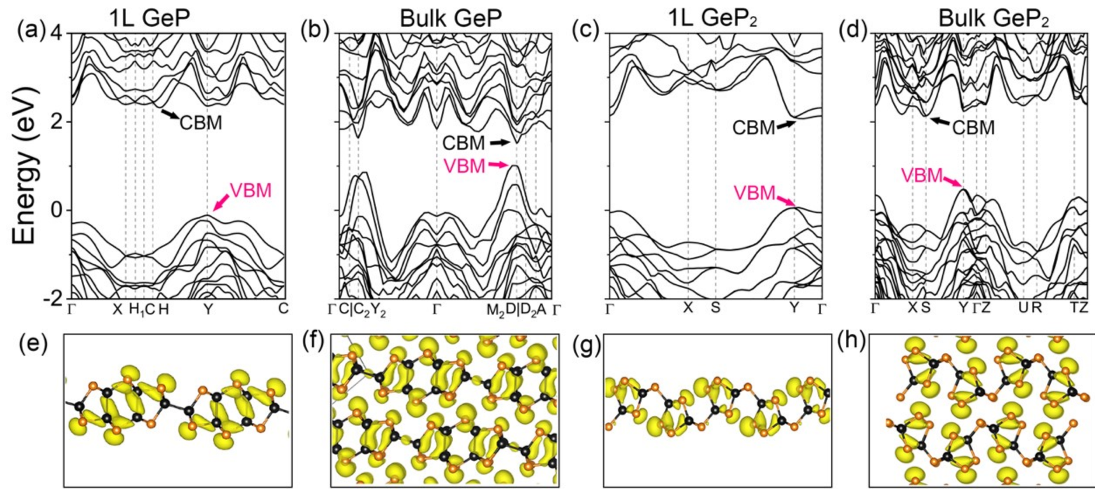

Figure S4. HSE06 calculated band structures and VBM partial charge densities of (a) 1L GeP, (b) bulk GeP, (c) 1L GeP_2 and (d) bulk GeP_2. Energy levels are aligned with respect to vacuum level, and the zero point of energy is situated at the Fermi level of 1L GeP.

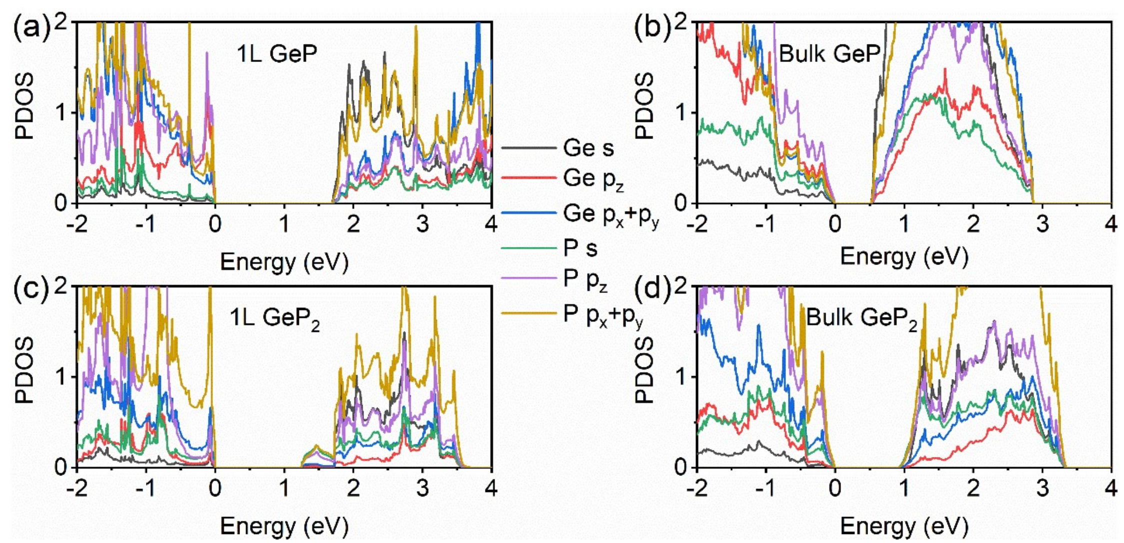

Figure S5. Partial density of states for (a, b) 1L and bulk GeP, respectively; (c, d) 1L and bulk GeP_2, respectively.

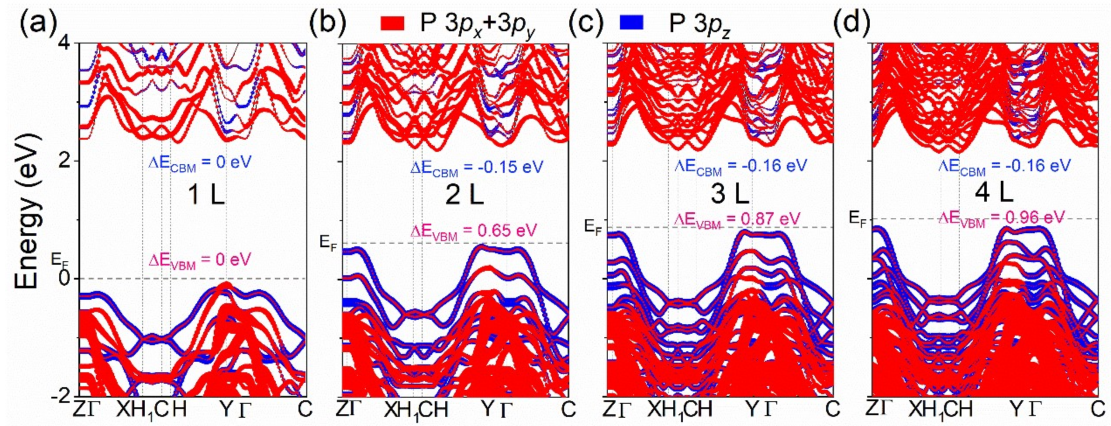

Figure S6. HSE06 calculated band structures of GeP of (a) monolayer (1L), (b) bilayer (2L), (c) trilayer (3L) and (d) quad-layer (4L), aligned based on the vacuum level (the Fermi level of 1L GeP is set as 0 eV).

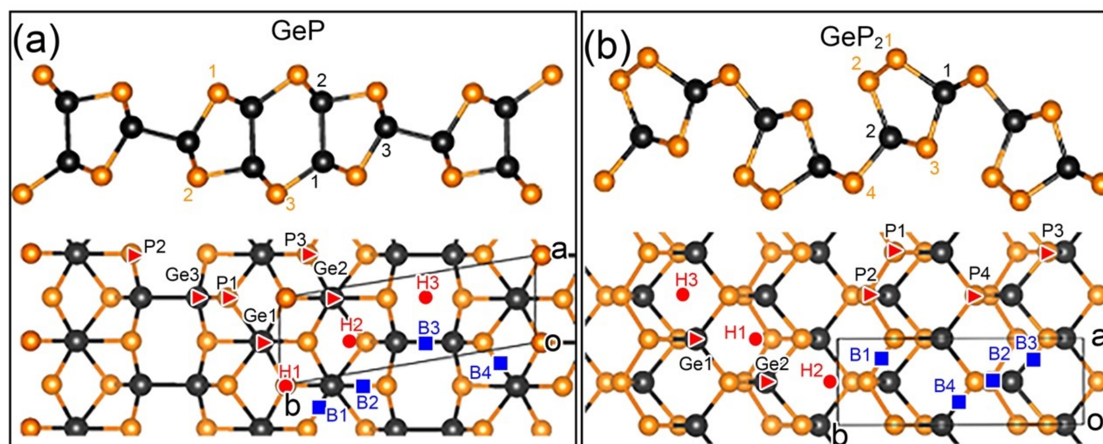

Figure S7. Schemes of sites for self-interstitials or adatoms in (a) GeP and (b) GeP_2.

Table S2. Relative energies of self-interstitials on different sites in GeP and GeP_2.

GeP			GeP_2		
Sites	Energy (eV)		Sites	Energy (eV)	
	Ge_i	P_i		Ge_i	P_i
Ge1	0.27	-	Ge1	-	-
Ge2	0.24	-	Ge2	-	-
Ge3	0.20	-	P1	0.82	1.18
P1	-	0.29	P2	-	-
P2	-	0.45	P3	-	-
P3	-	0.30	P4	0.83	1.26
B1	0.31		B1	0	0
B2	0.31	0	B2	1.04	1.07
B3	-	0.97	B3	1.14	1.58
B4	-	0.40	B4	1.45	-
H1	0.35	0.44	H1	1.09	1.33
H2	0.09	0.34	H2	0.47	0.86
H3	0	0.31	H3	0.81	-
In	0.73	0.96	In	-	-

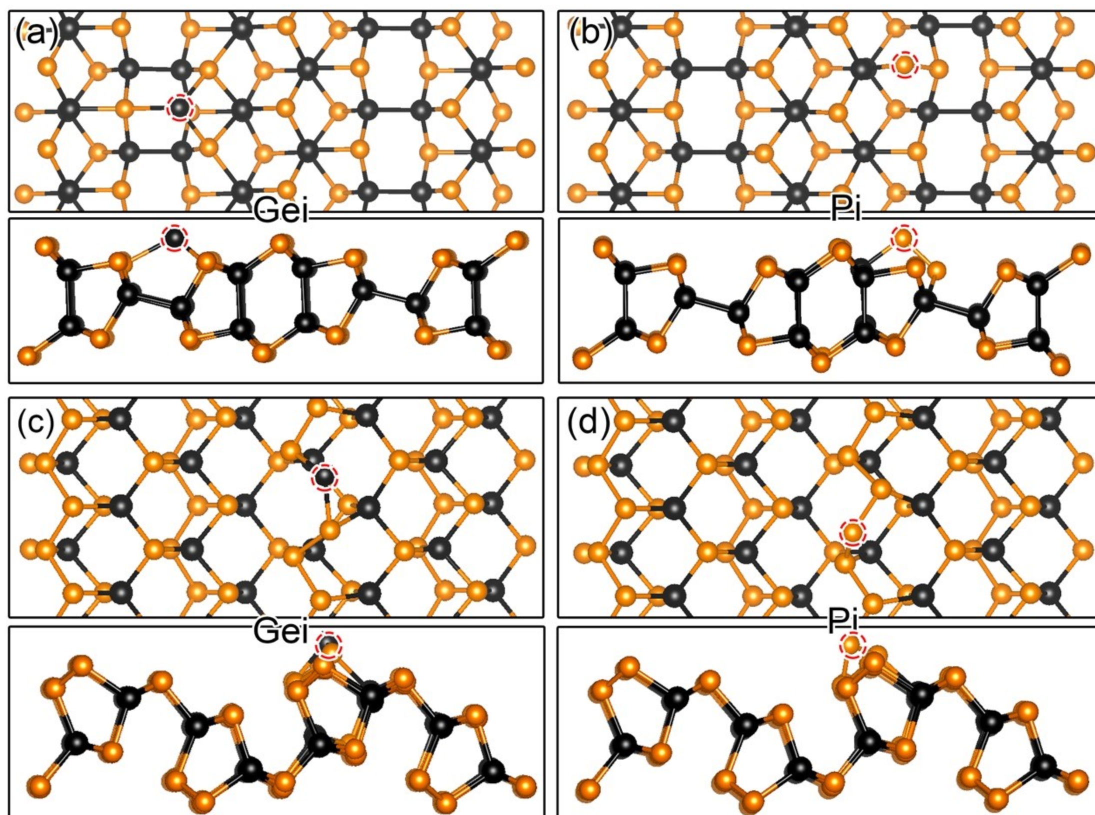

Figure S8. Atomic configurations of the most favorable sites for self-interstitials (a) Ge_i in GeP, (b) P_i in GeP, (c) Ge_i in GeP_2, and (d)P_i in GeP_2.

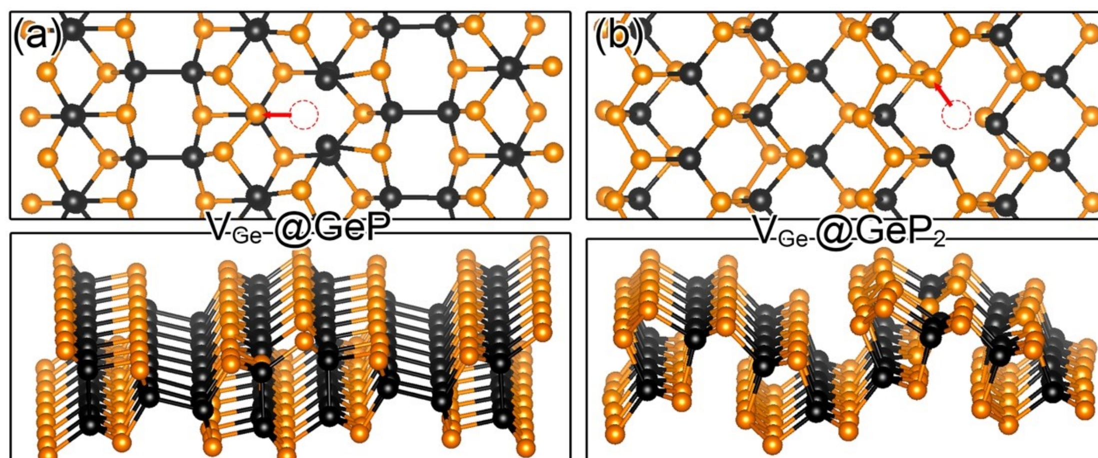

Figure S9. Atomic configurations of Ge vacancy (V_{Ge}) in (a) GeP and (b) GeP_2.

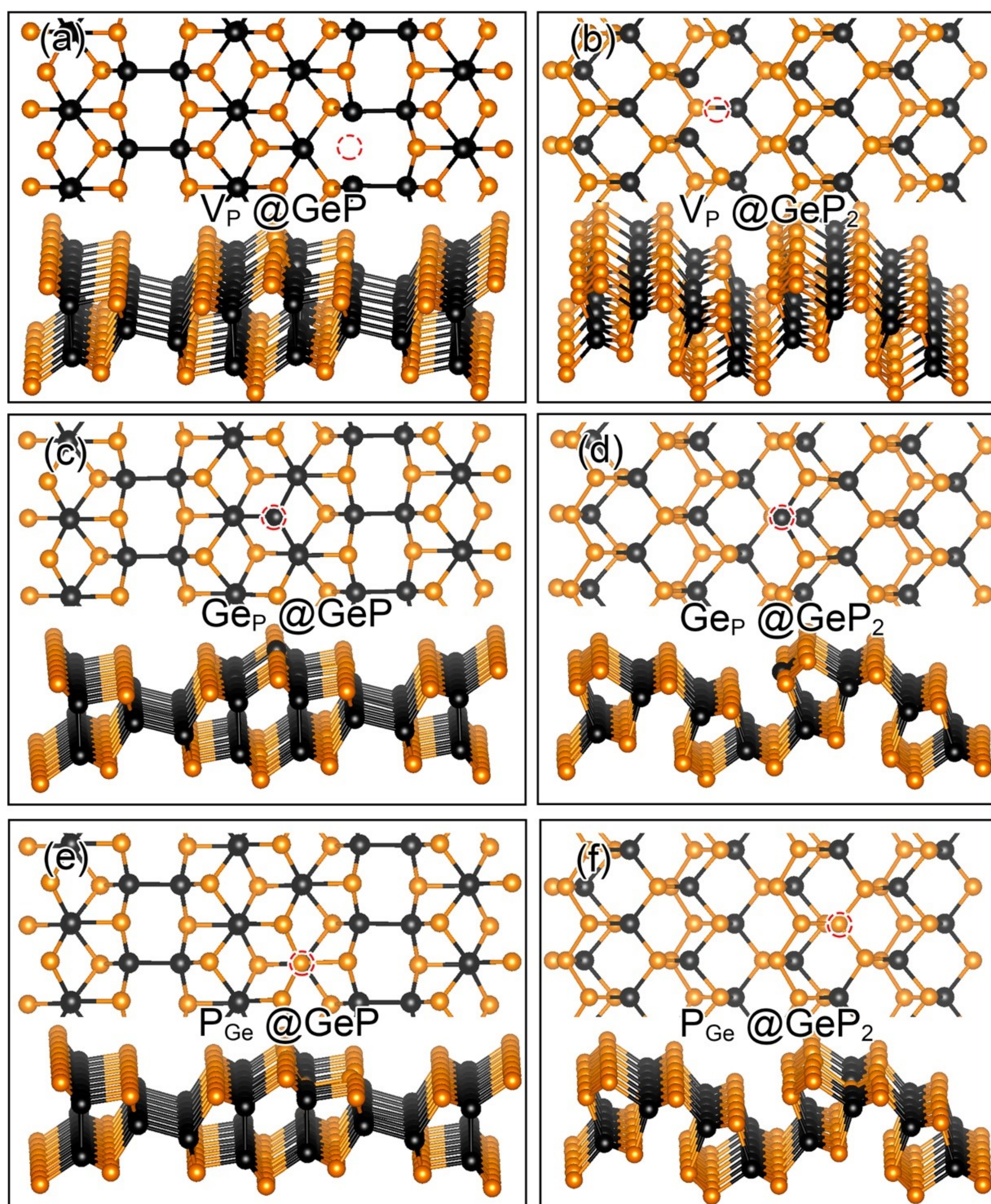

Figure S10. Atomic configurations of P vacancy (V_P) in (a) GeP and (b) GeP_2, antisite Ge_P in (c) GeP and (d) GeP_2, and antisite P_{Ge} in (e) GeP and (f) GeP_2.

Table S3. Interlayer-spacing, thickness of each layer and relative total energies of pristine and defective GeP and GeP_2 under fixed-supercell and full relaxations.

		Interlayer-spacing (Å)		Thickness of each layer (Å)		Energy (eV)	
		Fixed-supercell	Full-relaxed	Fixed-supercell	Full-relaxed	Fixed-supercell	Full-relaxed
GeP	Pristine	1.46	1.46	6.44	6.44	0	0
	Ge_{P3}	1.46	1.44	6.44	6.40	0	-0.02
	P_{Ge2}	1.43	1.42	6.44	6.42	0	-0.00(07)
GeP_2	Pristine	1.33	1.34	7.18	7.18	0	0
	Ge_{P2}	1.30	1.27	7.18	7.18	0	-0.04
	P_{Ge1}	1.33	1.32	7.18	7.19	0	-0.03

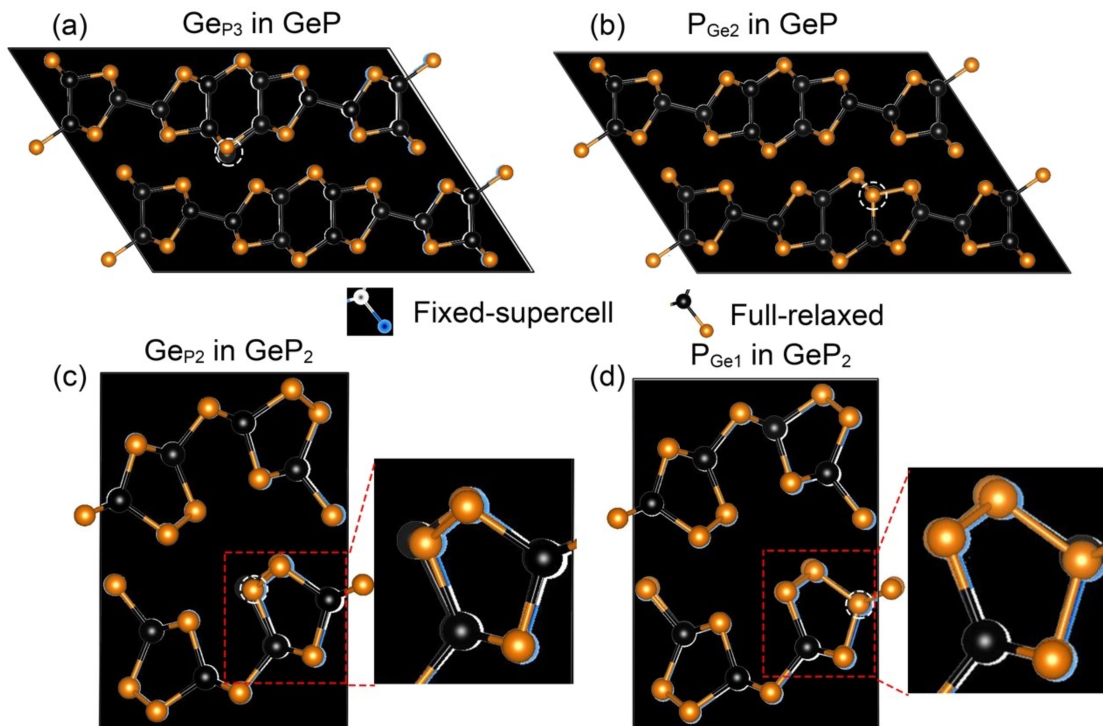

Figure S11. Comparison of relaxed structures with antisite defects under full-relaxed and fixed-supercell relaxed methods (white shadow indicating positions of atom under fixed-supercell relaxation).

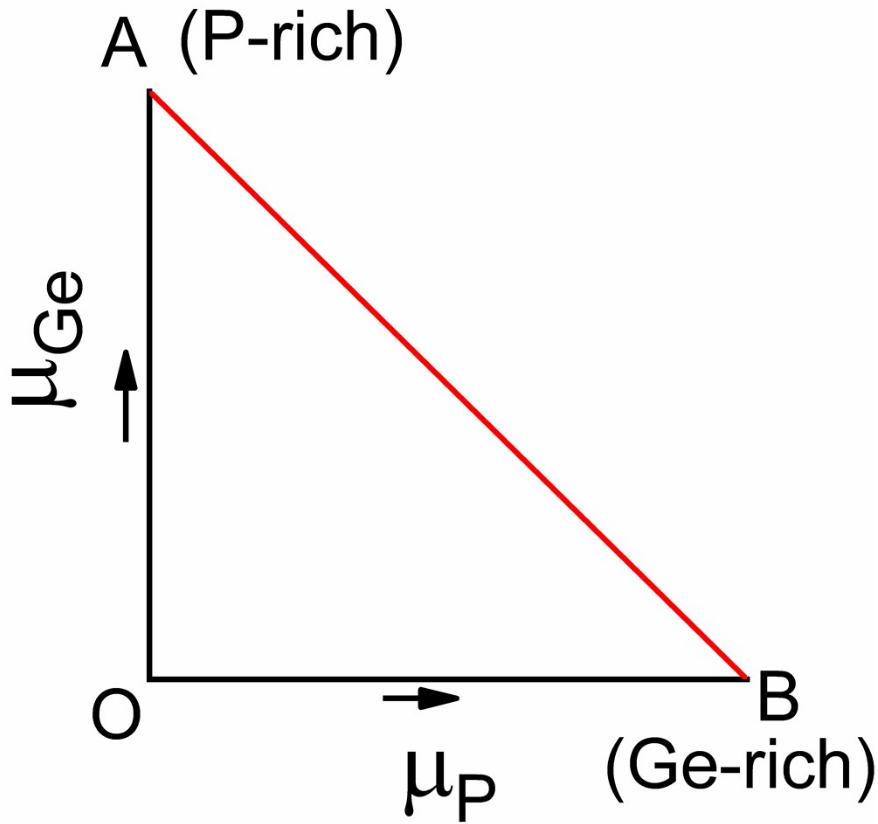

Figure S12. The chemical potential of host elements, μ_{Ge} and μ_P, satisfying the relation $\mu_{Ge} + \mu_P = \Delta H(GeP)$, in the range of the red line AB. Point A (P-rich, bulk GeP: μ_{Ge} = -0.03 eV and μ_P = 0 eV, monolayer GeP: μ_{Ge} = -0.03 eV and μ_P = 0 eV) and point B (Ge-rich, bulk GeP: μ_{Ge} = 0 eV and μ_P = -0.03 eV, monolayer GeP: μ_{Ge} = 0 eV and μ_P = -0.03 eV), are boundaries of PBE calculated chemical potential range. For the HSE06 calculated chemical potential range, point A (P-rich condition, bulk GeP: μ_{Ge} = -0.058 eV and μ_P = 0 eV, 1L GeP: μ_{Ge} = -0.055 eV and μ_P = 0 eV) and point B (Ge-rich condition, bulk GeP: μ_{Ge} = 0 eV and μ_P = -0.058 eV, 1L GeP: μ_{Ge} = 0 eV and μ_P = -0.055 eV) are boundaries.

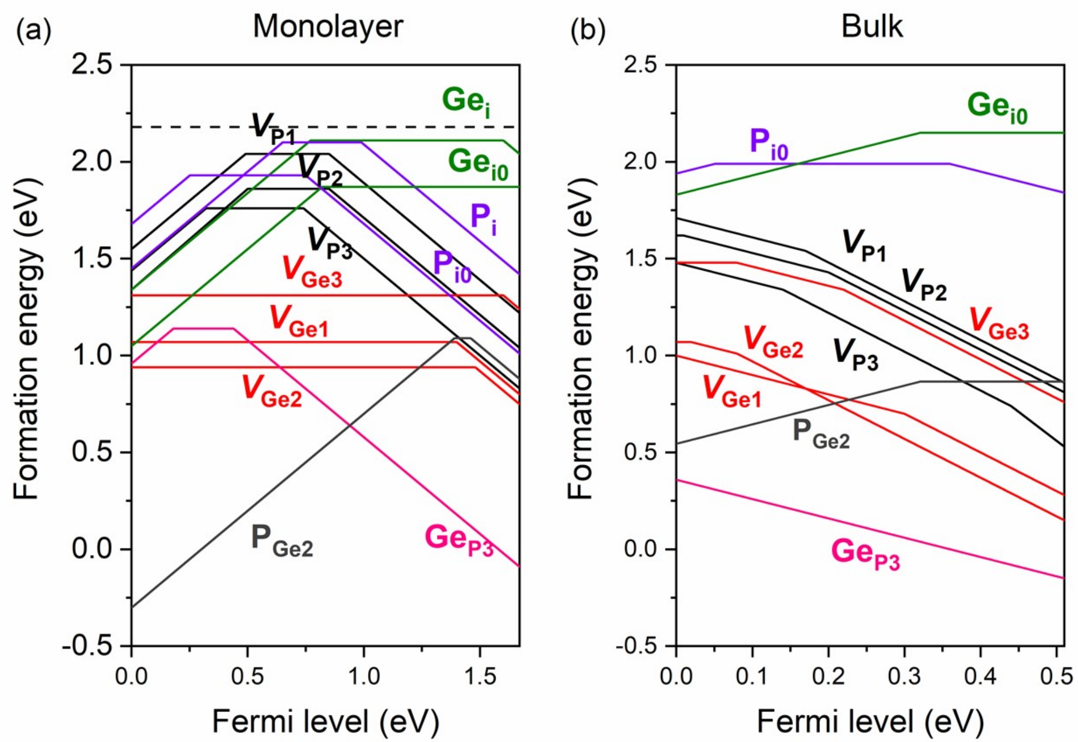

Figure S13. PBE calculated formation energy for all possible intrinic defects in (a) monolayer GeP and (b) bulk GeP at Ge-rich condition.

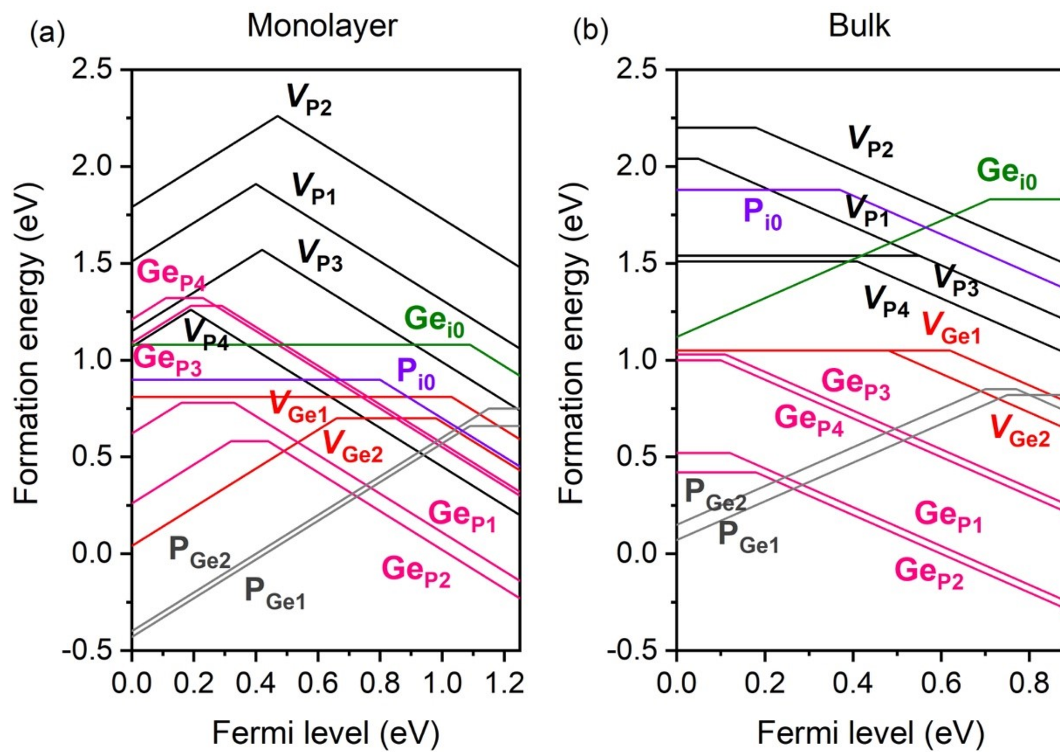

Figure S14. PBE calculated formation energy for all possible intrinsic defects in (a) monolayer GeP_2 and (b) bulk GeP_2 at Ge-rich condition.

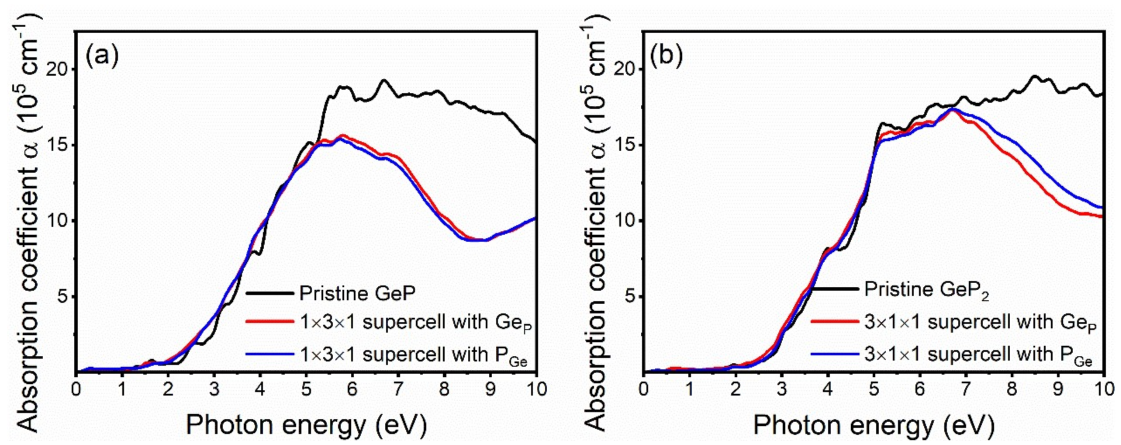

Figure S15. HSE06 calculated optical absorption coefficients of pristine and defective supercells (with antisites Ge_P and P_{Ge}) of (a) GeP and (b) GeP_2.

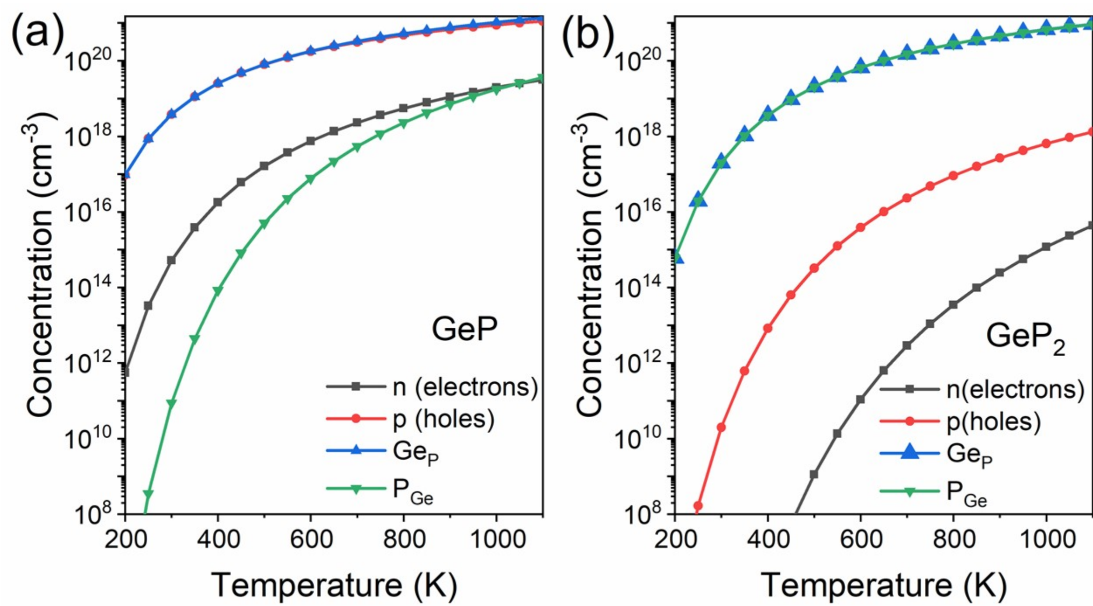

Figure S16. The carrier and defect concentrations as function of temperature for defects in bulk (a) GeP and (b) GeP_2.